Ultrafast dynamics in metallic and semiconducting carbon nanotubes

Larry Lüer,[1,2,*] Guglielmo Lanzani,[3] Jared Crochet,[4] Tobias Hertel,[4] Josh Holt,[5] and Z. Valy Vardeny[5]
[1]*CNR/INFM ULTRAS, Politecnico di Milano, 20133 Milano, Italy*
[2]*Madrid Institute of Advanced Studies, IMDEA Nanociencia, 28049 Madrid, Spain*
[3]*IIT-Dipartimento di Fisica, Politecnico di Milano, 20133 Milano, Italy*
[4]*Institut für Physikalische Chemie, Universität Würzburg, D-97070 Würzburg, Germany*
[5]*Physics & Astronomy Department, University of Utah, Salt Lake City, Utah 84112, USA*
(Received 11 July 2009; revised manuscript received 29 September 2009; published 10 November 2009)

Transient polarized pump/probe transmission changes upon pulse photoexcitation at 1.6 eV were measured in chiral enriched carbon nanotubes ensembles of both metallic and semiconductor characters, in a very broad probe spectral range from mid-IR to visible, combining several ultrafast laser systems. We identify a photoinduced absorption band at ~0.7 eV as due to hot Dirac fermions in the metallic tubes and measure its dynamics. The hot carriers equilibrate within the electronic system in ~400 fs and with the lattice within ~2 ps; in agreement with hot Dirac fermions thermalization in graphene. We also assign excitonic transitions in the semiconducting tubes, mainly of (6,5) chirality; in particular, an intraexciton transition at ~0.4 eV represents a lower limit for the exciton binding energy.

DOI: 10.1103/PhysRevB.80.205411 PACS number(s): 78.67.Ch, 73.22.−f, 78.47.J−

I. INTRODUCTION

Carbon nanotubes (NTs) are quasi-one-dimensional (1D) π-conjugated systems that possess a high potential for nanoscale optoelectronic devices.[1] It is well known that these materials exist in both semiconducting (S) and metallic (M) states, depending on their diameter and chirality. Due to the linear dispersion relation, M-NTs support low-energy exotic elementary excitations, dubbed Dirac fermions that have been most typically investigated in graphene, which are characterized in both 1D (tube) and two dimensional (2D) space (graphene) by a zero effective mass at low energies. Dirac fermion dynamics is object of intense investigation, predominantly in the 2D case.[2] However M-NT and their peculiar photoexcitations also play a crucial role in nanotubes *ensembles*, where they can act as energy and charge carrier traps for photoexcitations in S-NT. In spite of the substantial interest in Dirac fermions, spectroscopic techniques have so far limited impact on their study in NTs because the ensemble optical spectra are dominated by excitons in S-NTs, having strong and narrow optical resonances. The sharp optical resonances stem from the 1D confinement characteristic of the *e-h* dynamics, which leads to binding energies on the order of a few hundred meV (Refs. 3 and 4) and *e-h* correlation lengths of about 2 nm.[5,6] The oscillator strength in this case is concentrated in the lowest optically allowed excitonic transition and is essentially negligible for the band-to-band transition. As a result free *e-h* pairs *are not formed* in S-NT upon photon absorption. In M-NT, however, where *e-h* correlation has lesser impact,[7] absorption in the visible spectral range is due to band-to-band transitions involving valence (hole) and conduction (electrons) states, which lie below and above the Dirac point in the dispersion relation (see Fig. 1 inset). There is therefore an opportunity to study Dirac fermions and their distinct photoinduced features in CNT ensembles that contain abundant M-NT that can be preferentially excited.

Here we present a femtosecond pump-probe study of photoexcitation dynamics in chiral enriched, CoMoCAT NTs in matrix suspension. Transient transmission changes upon pulsed photoexcitation at 1.6 eV were measured in a very broad spectral range from the mid-IR to the visible, combining several laser systems. Combined with polarization memory decay measurements the measured transients allow us to identify an induced spectral feature at ~0.7 eV as due to Dirac fermion dynamics in M-NT. We found that the hot quasiparticles thermalize within the electronic system within ~400 fs, whereas thermalization with the lattice occurs within ~2 ps; both in agreement with Dirac fermions dy-

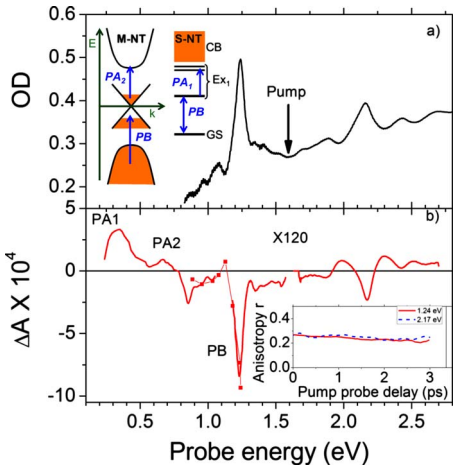

FIG. 1. (Color online) (a) Ground-state absorption spectrum of the Comocat CNT sample, where the excitation photon energy at 1.6 eV is assigned. Inset: energy level diagram and excited optical transitions for M-NT (left) and S-NT (right). Filled areas indicate fully occupied electronic states. For metallic nanotubes the first and second valence (conduction) bands are assigned, whereas for semiconducting nanotubes the $k=0$ exciton states and continuum band are shown. (b) Transient photomodulation spectrum at $t=0$ (within 200 fs) obtained using the MHz laser system (in the mid-IR and single data points) and the kHz system (near-IR-visible range), respectively; the signal for the latter was scaled down by a factor of 120 for normalization purpose. The inset shows the pump-probe anisotropy, $r(t)$ in the PB bands E^{11} and E^{22} of the (6,5) S-NT, obtained using the kHz system.

namics recently obtained in 2D graphene.[2] We also assign excitonic spectral features in SNT, mainly of (6,5) chirality; in particular, a prominent intraexciton transition around 0.4 eV represents a lower limit for the exciton binding energy.

We study films of CoMoCAT/Na-cholate NT suspensions obtained by density gradient ultracentrifugation.[8] The most abundant nanotube type is the (6,5) which accounts for about 45% of all S-NT. Recently, the fraction of M-NT in mixed metallic/semiconducting NTs has been measured to about 8%.[9] The individual NTs in our sample are organized in small bundles that are parallelly aligned to each other in a hexagonal Bravais lattice.

Transient polarized photomodulation (PM) spectroscopy in the mid-IR spectral range was carried out using a fs two-color pump-probe correlation technique with a low-power (energy/pulse ≈ 0.1 nJ), high repetition rate (≈ 80 MHz) laser system based on Ti:sapphire (Tsunami, Spectra-Physics) and an optical parametric oscillator (Opal, Spectra-Physics) with a probe frequency ranging from 0.24 to 1.1 eV. Pump-probe spectroscopy in the near-IR (NIR) to visible spectral range (0.9–2.7 eV) was performed using a regeneratively amplified, 1 kHz titanium-sapphire laser system with medium/strong power (energy/pulse ~ 100 nJ). We measured the transient change ΔT in transmission, T using a phase-sensitive technique; where the transient absorbance change, ΔA was obtained as $\Delta A \approx -\Delta T/T$. For both spectral regimes the linear dependence of ΔT on the pump pulse energy was confirmed. The PM spectra from the two laser systems were normalized within the spectral overlap from 0.90 to 1.25 eV. We also measured the transient polarization anisotropy, r defined by the relation $r=(\Delta A_{par}-\Delta A_{perp})/(\Delta A_{par}+2\Delta A_{perp})$, where ΔA_{par} and ΔA_{par} are ΔA with parallel and perpendicularly polarized pump and probe beams, respectively.

The ground-state absorption spectrum, shown in Fig. 1, is dominated by the two excitonic resonances of the (6,5) tube, at 1.24 and 2.17 eV for the E^{11} and E^{22} resonances, respectively. This spectrum also contains a broad background the origin of which is still under debate. It has been shown that higher excitonic states and residual oscillator strength from the free-carrier continuum can play a role.[3,10] The later might be enhanced by dielectric screening due to other tubes in the bundle. Upon excitation away from the sharp lines, the creation of free *e-h* pairs may be favored.

The transient PM spectrum at $t=0$ for excitation at 1.6 eV is shown in Fig. 1(b) from 0.25 to 2.8 eV. It shows two main negative features that corresponds to the excitonic resonances of the (6,5) tube and can thus be assigned to ground-state photobleaching (PB) caused by phase-space filling in the (6,5) tubes.[6] We note that compared to the absorption spectrum, the relative intensity of the PB bands between 0.80 and 1 eV [including the (15,1) tube] is larger. This is most likely due to excitation of tubes having E^{22} resonances near the 1.6 eV pump excitation but may also indicate energy migration within the NT bundle. The presence of PB features above the pump energy, notably the E^{22} resonance of the (6,5) tube, suggests strong electron correlation, leading to configuration interaction and transition mixing, similar to organic molecules.[11] In summary, the ΔA spectrum indicates that pumping at 1.6 eV predominantly leads to excitation of

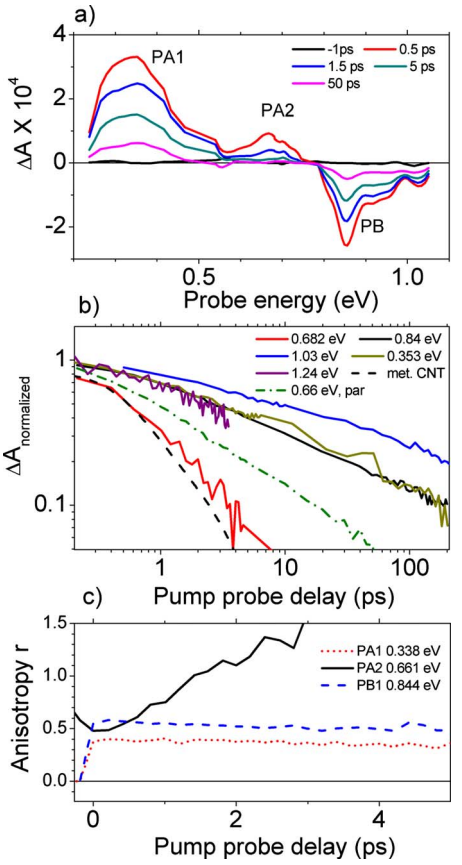

FIG. 2. (Color online) (a) Time-resolved PM spectra in the mid- and near-IR spectral range. (b) Normalized time decays, measured at various probe photon energies; the decay at 1.24 eV was obtained with the kHz system, whereas all other decays were obtained with the MHz system. All curves measured with perpendicular pump-probe polarization, except the trace labeled "par" (parallel polarization). Black dotted curve: calculated electronic cooling dynamics in M-NT using literature parameters (see text). (c) Transient anisotropies for the PA1, PA2, and PB bands obtained with the MHz system.

(6,5) tubes, owing to their high abundance in this sample, but photoexcitations in other tubes are also possible.

In Fig. 1(b) inset, we show the pump-probe transient polarization anisotropy $r(t)$ for the PB bands of the (6,5) tube at 1.27 and 2.17 eV, respectively, measured with the kHz laser system. We find a high polarization anisotropy ($r \approx 0.3$) that is approximately constant for both bands. Since the exciton transitions are polarized along the nanotube axis, this suggests that the transition which is excited at 1.6 eV is also polarized along the nanotube axis. This is consistent with conservation of dipole orientation during intertube energy transfer. A similar behavior is found for the transient polarization memory of trans-polyacetylene polymer chains, which can also arrange in nanofibrils.[12]

The mid-infrared PM spectrum is dominated by two photoinduced absorption (PA) bands, at 0.35 eV (PA1), and at 0.7 eV (PA2), respectively [Fig. 2(a)]. Both bands are formed instantaneously with the pump excitation, however, PA2 decays much faster than PA1. In Fig. 2(b), we show normalized transients at various probe energies, where the

PA1 and PA2 dynamics are compared to those of selected PB frequencies. We found PA1 dynamics perfectly matches that of PB of both $PB_{6,5}$ and $PB_{15,1}$ (at 1.24 and 0.86 eV, respectively, for the indexed chiralities). The kinetics follows a power-law form $y(t)=y_0t^{-\gamma}$, with $\gamma\approx 0.45$, which is typical for subdiffusive trapping.[8] Thus PA1 can be assigned to a transition from the lowest lying (1u) exciton state to a higher exciton state (2g), or to the *e-h* continuum. This establishes a lower limit for the exciton binding energy in the (6,5) tube $E_b > 0.35$ eV, consistent with theoretical calculations[5] and nonlinear optical measurements such as two-photon absorption (Ref. 4) as well as single nanotube fluorescence.[3]

As noted above, PA2 is much shorter lived than PA1. Its kinetics is well fitted by a biexponential decay function, having time constants $\tau_1 \sim 400$ fs and $\tau_2 \sim 2$ ps, respectively. Moreover, none of the PB features, associated with S-NT, shows this ultrafast decay component. Therefore PA2 does not come from S-NT in our sample. In fact similar kinetics to those of PA2 was measured in time-resolved photoemission and assigned to electron cooling in M-NT following optical excitation.[13] We thus conclude that PA2 is associated with M-NT. Additional evidence that this PA band involves M-NT, is obtained from its transient polarization. Figure 2(b) shows that the ultrafast decay occurs for PA2 only in the perpendicular pump/probe polarization; whereas the decay in the parallel polarization is much slower. As a result the anisotropy, r of PA2 band actually *rises* during the first few picoseconds [see Fig. 2(c)], whereas all other PA and PB bands have constant r close to the value 0.4 predicted for isotropically oriented transition dipoles. Theory predicts that optical transitions from Dirac fermions to higher bands be perpendicularly polarized.[14] We thus propose that PA2 is due to transitions involving hot Dirac fermions. For a summary of the band assignments to optical transitions in S-NT and M-NT, see inset of Fig. 1(a).

In order to identify the number of independent spectral components we perform a global fit of the time- and frequency-dependent data set. Specifically this allows singling out the contribution of fast decay processes to the transients at probe energies where a superposition of PA2, PA1, and PB bands seems likely (see Appendix for details). We left the rate constant and dispersive parameter γ of S-NT as free parameters in the fitting, whereas the corresponding parameters for M-NT were fixed to the value we found above. Figure 3 shows that the global fit describes all transient spectra [Fig. 3(a)] and cross correlations [Fig. 3(b)] very well. The calculated populations of the excited states in the various NT are shown in Fig. 3(d). All contributions from M-NT are found to decay within ~ 5 ps. The transient PM spectra, as obtained from the global fit are shown in Fig. 3(c). As expected, the principal components that correspond to S-NT can account for the majority of the PB and PA1 bands but show negligible spectral weight in the region of the PA2 band. The latter is dominated by the decay associated with metallic tubes. However, the global fit shows that the fast decay process is also present in the low-energy part of PA1. In fact, comparing the spectra for 0.2 and 2 ps in Fig. 3(a) confirms that the low-energy part of PA1 decays more quickly, leading to a change in the PA1 spectral shape during the first few picoseconds. Moreover, the fastest process (with 0.4 ps lifetime, red (dark gray) line in Figs. 3(c) and 3(d)) has a strong contribution to the PB region at 0.86 eV. This suggests that PA2 is part of a first-derivative shaped time-dependent spectrum with positive and negative contributions. Such features are typically obtained in transient spectra of metals and describe electron-gas cooling in the vicinity of the Fermi level.[13] This corroborates our assignment of fast dynamics to cooling at the Dirac point in metallic nanotubes. A schematic representation of the predicted optical transitions in S-NT and M-NT is given in the inset of Fig. 1(a); for M-NT excited at 1.6 eV, the optical band gap for the (perpendicularly polarized) transition from the Fermi edge to the first exciton band is expected at around 0.8 eV. A nonequilibrium distribution of the Fermions will thus result in additional absorption below 0.8 eV, together with a bleach above 0.8 eV, in accordance with the results from the global fit.

The transient response of Dirac fermions in multilayer graphene was recently reported.[2] The transients were also found to follow a biexponential decay function with two-time constants, very similar to τ_1 and τ_2 obtained here. The fast time constant of few hundred fs was interpreted as due to hot carrier thermalization within the electronic systems establishing a quasiequilibrium electronic temperature, $T_e > T$; whereas the longer, ps time constant was assigned to cooling of the electron plasma, where the electronic temperature, T_e approaching that of the lattice temperature. Similarly we interpret the obtained time constant τ_1 as due to hot carrier thermalization within the electronic system and τ_2 as the time for the electronic and lattice subsystems to equilibrate. We thus conclude that in fact the Dirac fermion dynamics are not different in 1D M-NT and 2D graphene.

In conclusion, by probing a very broad spectral region in the NIR-visible range we assign a fast PA band as due to Dirac Fermion cooling. We identify a spectral signature of these states in the transient PM spectra and measure their cooling rate in 1D metals, reporting a quantitative description. The extremely fast kinetics, described by a biexponential with 0.4 and 2 ps time constant, respectively, are interpreted as due to hot carrier thermalization to establish an electronic temperature and plasma cooling to the lattice. In addition, we also found a low-energy PA band at 0.35 eV, which seems common to excitons in S-NT and suggests a lower limit for their binding energy.

ACKNOWLEDGMENTS

This work was financially supported by the European Commission through the Human Potential Program (Marie-Curie RTN BIMORE, Grant No. MRTN-CT-2006-035859) and by the National Science Foundation (Grant No. NSF DMR-0606505).

APPENDIX: GLOBAL FIT

The time-dependent populations relative to semiconducting (sc), excited metallic (m), and electronically hot (h) metallic tubes are found by numerically solving the following rate equations:

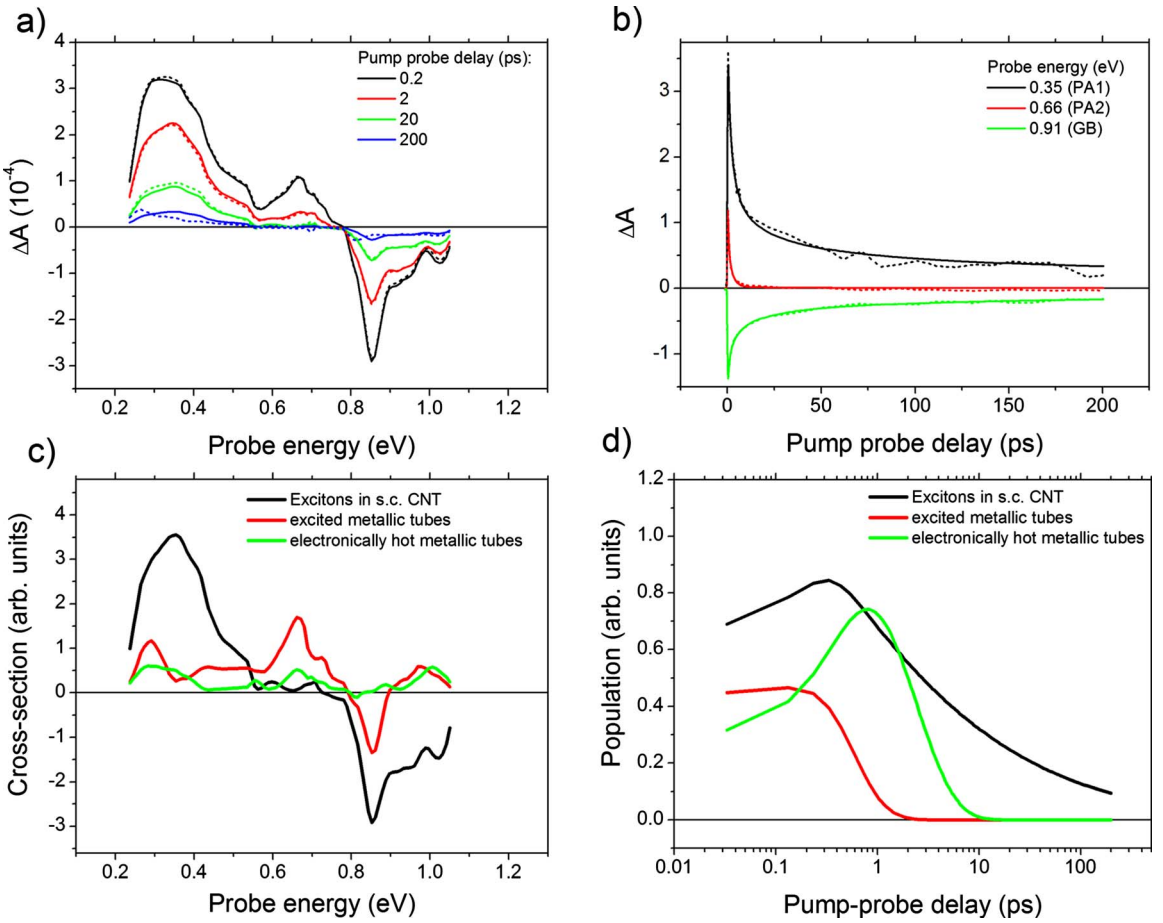

FIG. 3. (Color online) Global fit of time-resolved PM spectra, assuming three different types of photoexcitations (a) single spectra at various pump-probe delay times given in the box (thin dotted curves) and global fits (thick solid curves). (b) Single time traces in the PA1, PA2, and PB bands at given probe energies (thin dotted curves) and global fits (thick solid curves). (c) Absorption cross-section spectra for the photoexcitations, as obtained from the global fitting routine. (d) Time-dependent populations of the photoexcitations as obtained from the global fitting routine.

$$\left\{\begin{aligned}\frac{dn_{\mathrm{sc}}}{dt} &= g(t) - k_1(t)n_{\mathrm{sc}} \\ \frac{dn_{\mathrm{m}}}{dt} &= g(t) - k_r n_{\mathrm{m}} \\ \frac{dn_{\mathrm{h}}}{dt} &= k_r n_{\mathrm{m}} - k_c n_{\mathrm{h}}\end{aligned}\right\}.$$

We fixed the electronic relaxation time $1/k_r$ and the electronic cooling time $1/k_c$ to 0.4 and 2.0 ps, respectively. Exciton decay in the semiconducting tubes was assumed dispersive, $k_1(t)=k_{1,0}(t/t_0)^{\gamma}$ *with* $t_0=1$ ps. The optical generation of excited states occurs with the Gaussian generation function $g(t)$. The global fitting procedure is done by minimizing the error square between the measured matrix, $\Delta A_{\mathrm{exp}}(E,t)$ and the calculated one, $\Delta A_{calc}(E,t) = d\Sigma_i \sigma(i,E)c(i,t)$ by optimizing the absorption cross sections $\sigma(i,E)$ and the populations $c(i,t)$ for all photoexcitations $i \in \{\mathrm{sc},\mathrm{m},\mathrm{h}\}$ as defined in the kinetic equation scheme. The film thickness is given by d.

*larry.luer@imdea.org

[1] P. Avouris, Z. H. Chen, and V. Perebeinos, Nat. Nanotechnol. **2**, 605 (2007).

[2] P. A. George, J. Strait, J. Dawlaty, S. Shivaraman, M. Chandrashekhar, F. Rana, and M. G. Spencer, Nano Lett. **8**, 4248 (2008).

[3] J. Lefebvre and P. Finnie, Nano Lett. **8**, 1890 (2008).

[4] F. Wang, G. Dukovic, L. E. Brus, and T. F. Heinz, Science **308**, 838 (2005).

[5] R. B. Capaz, C. D. Spataru, S. Ismail-Beigi, and S. G. Louie, Phys. Rev. B **74**, 121401 (2006).

[6] L. Luer, S. Hoseinkhani, D. Polli, J. Crochet, T. Hertel, and G. Lanzani, Nat. Phys. **5**, 54 (2009).

[7] F. Wang, D. J. Cho, B. Kessler, J. Deslippe, P. J. Schuck, S. G.

Louie, A. Zettl, T. F. Heinz, and Y. R. Shen, Phys. Rev. Lett. **99**, 227401 (2007).
[8] Z. P. Zhu, J. Crochet, M. S. Arnold, M. C. Hersam, H. Ulbricht, D. Resasco, and T. Hertel, J. Phys. Chem. C **111**, 3831 (2007).
[9] A. V. Naumov, O. A. Kuznetsov, A. R. Harutyunyan, A. A. Green, M. C. Hersam, D. E. Resasco, P. N. Nikolaev, and R. B. Weisman, Nano Lett. **9**, 3203 (2009).
[10] A. Nish, J. Y. Hwang, J. Doig, and R. J. Nicholas, Nat. Nanotechnol. **2**, 640 (2007).
[11] L. Luer, C. Manzoni, G. Cerullo, G. Lanzani, and M. Meneghetti, Phys. Rev. Lett. **99**, 027401 (2007).
[12] Z. Vardeny, J. Strait, D. Moses, T. C. Chung, and A. J. Heeger, Phys. Rev. Lett. **49**, 1657 (1982).
[13] T. Hertel and G. Moos, Phys. Rev. Lett. **84**, 5002 (2000).
[14] Z. D. Wang, D. Psiachos, R. F. Badilla, and S. Mazumdar, J. Phys.: Condens. Matter **21**, 095009 (2009).